Activity From Magnetar Candidate 4U 0142+61: Bursts and Emission Lines

Fotis P. Gavriil[*,†], Rim Dib[**] and Victoria M. Kaspi[**]

[*]*NASA Goddard Space Flight Center, Astrophysics Science Division, Code 662, Greenbelt, MD, 20771, USA*
[†]*CRESST; University of Maryland Baltimore County, Baltimore, MD, 21250, USA*
[**]*Department of Physics, McGill University, Montreal, QC, H3A 2T8, Canada*

Abstract. After 6 years of quiescence, Anomalous X-ray Pulsar (AXP) 4U 0142+61 entered an active phase in 2006 March that lasted several months. During the active phase, several bursts were detected, and many aspects of the X-ray emission changed. We report on the discovery of six X-ray bursts, the first ever seen from this AXP in ~10 years of *Rossi X-ray Timing Explorer* monitoring. All the bursts occurred in the interval between 2006 April 6 and 2007 February 7. The burst durations ranged from $8-3\times10^3$ s as characterized by T_{90}. These are very long durations even when compared to the broad T_{90} distributions of other bursts from AXPs and Soft Gamma Repeaters (SGRs). The first five burst spectra are well modeled by simple blackbodies, with temperature $kT\sim2-6$ keV. However, the sixth and most energetic burst had a complicated spectrum consisting of at least three emission lines with possible additional emission and absorption lines. The most significant feature was at ~ 14 keV. Similar 14-keV spectral features were seen in bursts from AXPs 1E 1048.1–5937 and XTE J1810–197. If this feature is interpreted as a proton cyclotron line, then it supports the existence of a magnetar-strength field for these AXPs. Several of the bursts were accompanied by a short-term pulsed flux enhancement. We discuss these events in the context of the magnetar model.

Keywords: anomalous X-ray pulsar, magnetar, neutron star
PACS: 97.60.Gb, 98.70.Qy, 97.60.Jd

INTRODUCTION

Anomalous X-ray Pulsars (AXPs) are isolated neutron stars that show pulsations in the narrow range of 2–12 s. Their observed 2-10 keV X-ray luminosities ($\sim 10^{33}-10^{35}$ erg s^{-1}) cannot be accounted for by their available spin-down energy. It is widely accepted that AXPs are magnetars – young isolated neutron stars powered by their high magnetic fields [1, 2]. The inferred surface dipolar magnetic fields of AXPs are all above 5.9×10^{13} G. The magnetar model was first proposed to explain Soft Gamma Repeaters (SGRs). SGRs show persistent properties similar to AXPs, but they were first discovered by their enormous bursts of soft gamma rays ($>10^{44}$ erg) and their much more frequent, shorter, and thus less energetic bursts of hard X-rays. To date, SGR-like X-ray bursts have been observed from four AXPs, thus solidifying the connection between the two source classes [3, 4, 5, 6]. For a review of magnetar candidates see Woods and Thompson [7].

Thus far, only the magnetar model can explain the bursts observed from SGRs and AXPs [1]. The internal magnetic field exerts stresses on the crust which can lead to large scale rearrangements of the external field, which we observe as giant flares. If the stress is more localized, then it can fracture the crust and displace the footpoints of the external magnetic field which results in short X-ray bursts. The highly twisted internal magnetic field also slowly twists up the external field and it is believed that the magnetospheres of magnetars are globally twisted [8]. Reconnection in this globally twisted magnetosphere has also been proposed as an additional mechanism for the short bursts [9].

In addition to bursts, AXPs and SGRs exhibit pulsed and persistent flux variations on several timescales. An hours-long increase in the pulsed flux has been seen to follow a burst in AXP 1E 1048.1–5937 [10]. On longer timescales, AXPs can exhibit abrupt increases in flux which decay on ~week-month timescales. These occur in conjunction with bursts and are thought to be due to thermal radiation from the stellar surface after the deposition of heat from bursts. Such flux enhancements have been observed in SGRs (see Woods et al. [11] for example). The flux enhancement of AXP 1E 2259+586 during its 2002 outburst was also interpreted as burst afterglow [12], however, a magnetospheric interpretation has also been proposed [13]. AXP 1E 1048.1–5937 exhibited three unusual flux flares. In the first two, the pulsed flux rose on week-long timescales and subsequently decayed back on time scales of months [14, 15]. Although small bursts sometimes occur during these events [10], burst afterglow cannot explain the flaring, thus these variations have been attributed to twists implanted in the external magnetosphere from stresses on the crust imposed by the internal magnetic field. AXPs XTE J1810–197 and the AXP candidate AX J1845–0258 have also exhibited flux

CP983, *40 Years of Pulsars –Millisecond Pulsars, Magnetars, and More*,
edited by C. G. Bassa, Z. Wang, A. Cumming, and V. M. Kaspi,

variations, however it is not clear whether these were of the abrupt rise type as in 1E 2259+586 or the slow-rise type as in 1E 1048.1–5937. Finally, AXP 4U 0142+61 has exhibited the longest timescale flux variations, in which the pulsed flux increased by 19±9% over a period of 2.6 years [16].

ANALYSIS AND RESULTS

All data presented here are from the Proportional Counter Array (PCA) aboard the *Rossi X-ray Timing Explorer* (*RXTE*). The PCA is made up of five identical and independent proportional counter units (PCUs). Each PCU is a Xenon/methane proportional counter with a propane veto layer. The data were collected in either `GoodXenonwithPropane` or `GoodXenon` mode which record photon arrival times with ∼1-μs resolution and bins them with 256 spectral channels in the ∼2-60 keV band.

Burst Analysis

We have been monitoring 4U 0142+61 with the PCA for nearly a decade. Currently, it is observed bi-monthly with a typical observation length of 5 ks. For each monitoring observation of 4U 0142+61, using software that can handle the raw telemetry data, we generated 31.25 ms lightcurves using all Xenon layers and only events in the 2–20 keV band. These lightcurves were searched for bursts using our automated burst search algorithm introduced in Gavriil et al. [3] and discussed further in Gavriil et al. [17]. In an observation on 2006 April 6, we detected a significant burst, and four more bursts were detected in a single observation on 2006 June 25. The sixth and most energetic burst was detected on 2007 February 7. There were 3, 3, and 2 PCUs on at the times of the bursts for the April, June and February observations, respectively. The bursts were significant in each active PCU.

To further analyze these bursts we created event lists in FITS[1] format using the standard `FTOOLS`[2]. For consistency with previous analysis of SGR/AXP bursts we extracted events in the 2-60 keV band. These events were barycentered using the position found by Patel et al. [18] for the source. The burst lightcurves are displayed in Fig. 1.

Before measuring any burst parameters we determined the instrumental background using the `FTOOL` `pcabackest`. We extracted a background model lightcurve using the appropriate energy band and number of PCUs. `pcabackest` only determines the background on 16 s time intervals, so we interpolated these values by fitting a polynomial of order 6 to the entire observation, which yielded a good fit for each observation.

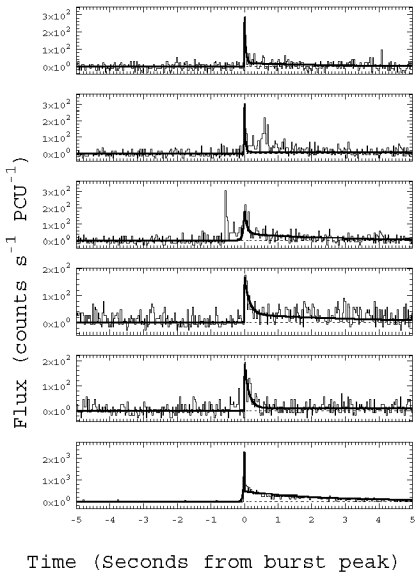

FIGURE 1. The histograms are the 2–60 keV burst lightcurves binned with 1/32 s resolution as observed by *RXTE*. The thick curves are the best fit exponential rise and exponential decay model.

The burst peak time, rise time and peak flux were determined using the methods described in Gavriil et al. [17]. Usually, to measure the fluence for SGR and AXP bursts, we subtract the instrumental background for the lightcurve, integrate the light curve and fit it to a step function with a linear term whose slope is the "local" background rate. The fluence in this case is the height of the step function. Although this technique worked well for the first burst, which was a short isolated event, it was not appropriate for bursts 2, 3, and 4 because they had overlapping tails, and bursts 5 and 6 had tails that extended beyond the end of the observation. Thus, we opted to fit the bursts to exponential rises with decaying tails. Our model fits are overplotted on the bursts in Fig. 1. As is done for γ-ray bursts and SGR and AXP bursts, we characterized the burst duration by T_{90}, the time from when 5% to 95% of the total burst counts have been collected. To determine the T_{90} duration we integrated our burst model and numerically determined the 5% and 95% time crossings. All burst temporal parameters are presented in Table 1.

Burst spectra were extracted using all the counts

[1] `http://fits.gsfc.nasa.gov`
[2] `http://heasarc.gsfc.nasa.gov/docs/software/ftools/`

TABLE 1. Burst Temporal and Spectral Properties

	April 2006	June 2006				February 2007
Parameter*	**Burst 1**	**Burst 2**	**Burst 3**	**Burst 4**	**Burst 5**	**Burst 6**
Burst day (MJD UTC)	53831	53911	53911	53911	53911	54138
Burst start time (UT)	07:09.55.544(7)	01:15:54.555(11)	01:15:55.119(43)	01:16:9.216(4)	01:20:0.131(3)	10:04:43.264(27)
Burst rise time, t_r (ms)	7^{+4}_{-3}	11^{+4}_{-3}	43^{+22}_{-22}	4^{+3}_{-3}	3^{+3}_{-1}	27^{+4}_{-3}
Burst duration, T_{90} (s)	$8.0^{+2.5}_{-2.2}$	$562.2^{+0.15}_{-0.15}$	$6.44^{0.15}_{-0.15}$	$11.62^{+0.15}_{-0.15}$	$92.54^{0.70}_{-0.85}$	$3472.9^{3.3}_{-3.4}$
T_{90} Fluence (counts PCU^{-1})	65±6	1847±4	125±9	147±8	342±9	14377±41
T_{90} Fluence ($\times 10^{-10}$erg cm^{-2})	16±3	229±11	26±3	38±3	43±4	1455±53
Peak Flux (counts s^{-1} PCU^{-1})	299±59	367±65	250±54	228±52	245±54	551±97
Peak Flux ($\times 10^{-10}$ erg s^{-1} cm^{-2})	75±19	46±8	53±12	58±14	31±7	253±22
Blackbody Temperature, $kT^{\dagger}$(keV)	$6.2^{+4.4}_{-1.9}$	$2.67^{+0.10}_{-0.09}$	$4.50^{+0.38}_{-0.29}$	$5.16^{+0.44}_{-0.34}$	$2.52^{+0.21}_{-0.13}$	$2.12^{+0.08}_{-0.04}$

* All quoted errors represent 1-σ uncertainties.

† For burst 6, the temperature is that of the blackbody component after accounting for the emission lines.

within their T_{90} interval. Background intervals were extracted from long, hand-selected intervals prior to the bursts. Response matrices were created using the FTOOL pcarsp. The burst spectra were grouped such that there were at least 15 counts per bin after background subtraction. Burst spectra, background spectra, and response matrices were then read into the spectral fitting package XSPEC[3] v12.3.1. The spectra were fit to photoelectrically absorbed blackbodies using the column density found by Durant and van Kerkwijk [19]. Only bins in the 2–30 keV band were included in the fits. The blackbody model provided an adequate fit for bursts 1 through 5. burst 6, however, was not well modeled by any simple continuum model because of the presence of emission lines (see Fig.2 panels 1A and 1B). These features showed clear temporal variability but they were most prominent near the onset of the burst (see Fig. 3).

Pulsed Flux Analysis

For each of the three observations containing bursts, we made two barycentered time series in count rate per PCU, one for the 2−4 keV band and the other for 4−20 keV. We only included the photons detected by the PCUs that were on for the entire duration of the observation. The time resolution was 1/32 s. We removed the 4 s centered on each burst from each time series. Then, we broke each time series into segments of length ∼500 s. For each segment, we calculated the pulsed flux using two different methods.

First, we calculated the RMS pulsed flux using the Fourier decomposition method described by Woods et al. [12], only incorporating the contribution of the first 5 harmonics for consistency with [16] and [20]. While least sensitive to noise, the RMS method returns a pulsed flux number that is affected by pulse profile changes (Archibald et al. in prep.). So to confirm our pulsed flux results, we also used an area-based estimator to calculate the pulsed flux, $PF = a_0 - \frac{p_{\rm min}}{N}$, where $a_0 = \frac{1}{N}\sum_{i=1}^{N} p_i$, i refers to the phase bin, N is the total number of phase bins, p_i is the count rate in the $i^{\rm th}$ phase bin of the pulse profile, and $p_{\rm min}$ is the average count rate in the off-pulse phase bins of the profile, determined by cross-correlating with a high signal-to-noise template, and calculated in the Fourier domain after truncating the Fourier series to 5 harmonics. The results are shown in Figure 4. Note the significant increase in the 4−20 keV pulsed flux in the 2007 June observation following the cluster of bursts. This increase is not present in 2−4 keV. Also note the significant rise and subsequent decay of the pulsed flux

[3] http://xspec.gsfc.nasa.gov

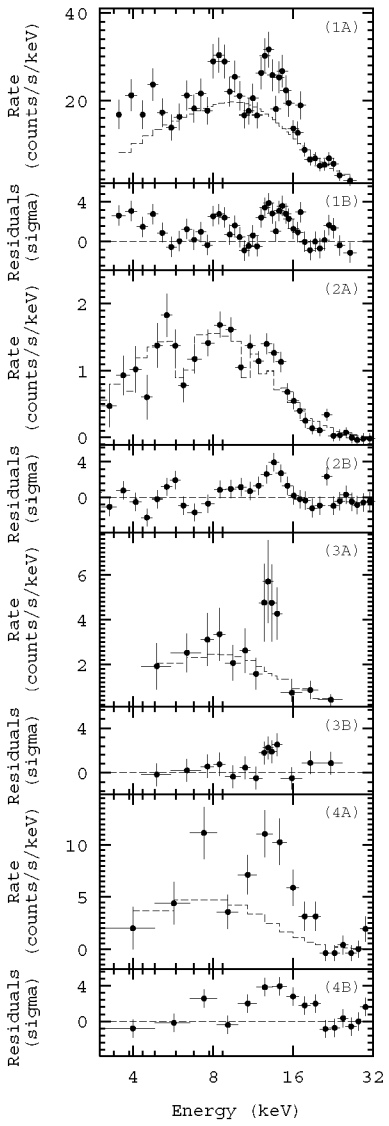

FIGURE 2. Burst spectra of all AXP bursts with significant emission lines as observed by *RXTE*. (1A) Burst spectrum of 4U 0142+61 burst 6. The dotted line indicates the continuum (blackbody) component of the best fit model. 1B: Residuals after subtracting the continuum component of the best fit model. 2A and 2B: Same but for burst 4 of XTE J1810–197 [see 5]. 3A and 3B: Same, but for burst 3 of 1E 1048.1–5937 [see 10]. 4A and 4B: Same, but for burst 1 of 1E 1048.1–5937 [see 3].

following the large 2007 February burst.

DISCUSSION

We have discovered six bursts from AXP 4U 0142+61. These bursts all occurred between 2006 April and 2007 February, and were the only ones ever observed from

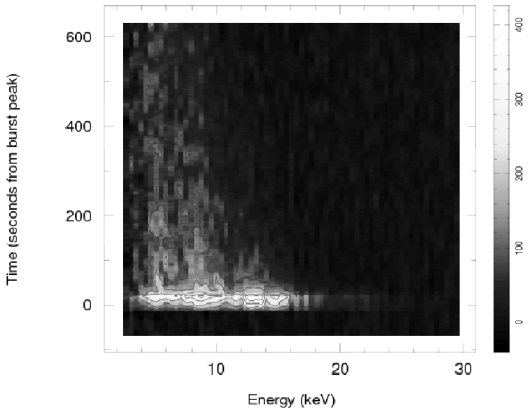

FIGURE 3. Dynamic spectrum of burst 6. The wedge indicates the number of counts as a function of time and energy. Notice how at later times the contribution of the features at ~4 keV and ~8 keV exceed that of the 14 keV feature.

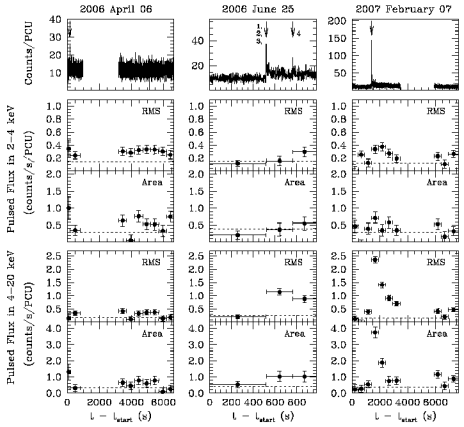

FIGURE 4. RMS and area pulsed flux within the observations containing bursts. Each column corresponds to one observation. In each column we have, descending vertically, the 1-s resolution lightcurve with the bursts indicated, the 2–4 keV RMS pulsed flux, the 2–4 keV area pulsed flux, the 4–20 keV RMS pulsed flux, and the 4 20 keV area pulsed flux. The dotted line in each of the pulsed flux plots shows the average of the pulsed fluxes obtained after segmenting and analyzing the time series of the observation immediately prior to the one shown.

this source in ~10 years of monitoring. After the first burst 4U 0142+61 exhibited a timing anomaly and pulse profile variations (Gavriil, Dib, & Kaspi in preparation). Together with the short-term pulsed flux increase, the simultaneity of all these phenomena clearly identifies 4U 0142+61 as the origin of the bursts.

Woods et al. [5] first argued that there appear to be two classes of magnetar bursts. Type A bursts are short, symmetric, and occur uniformly in pulse phase. Type B bursts have long tails, thermal spectra, and occur prefer-

entially at pulse maximum. Woods et al. [5] noted that type A bursts occur predominately in SGRs and type B bursts occur predominately in AXPs, and this was affirmed by Gavriil et al. [10]. Both argue that Type A and Type B bursts are produced by different mechanisms. In the magnetar model bursts can either be due to the rearrangement of magnetic field lines anchored to the surface after a crustal fracture [1], or due to reconnection in the upper magnetosphere [9]. Woods et al. [5] and Gavriil et al. [10] argue that Type B bursts are due to the former and Type A bursts are due to the latter. The bursts reported here all had very long tails, $T_{90} > 8$ s, suggesting they are of Type B. However, the bursts did not occur preferentially at pulse maxima.

The line-rich spectrum of burst 6 is intriguing. Three significant features are seen at ~4, ~8 and ~14 keV. The most significant emission feature at ~14 keV is particularly interesting. Emission features at similar energies were observed from two out of the three bursts from 1E 1048.1–5937 [3, 10] and in one out of the four bursts from XTE J1810–197[3, 5]. We have reanalyzed these burst spectra in a consistent manner as for 4U 0142+61. In Fig. 2 we plot the spectra of all AXP bursts with emission lines in their spectra. Notice that all the spectra have features that occur between 13 and 14 keV and are very broad. There is clear evidence for features at ~4 and ~8 keV in the 4U 0142+61 burst; however, note that there is subtle evidence for these features in some of the other burst spectra as well.

If the ~14 keV feature is interpreted as a proton cyclotron feature then we can infer the surface magnetic field strength of the star. For a line of energy E the magnetic field strength is given by

$$B = \left(\frac{mc}{\hbar e}\right) E. \quad (1)$$

Setting m equal to the proton mass we obtain $B = 2.2 \times 10^{15}\,(E/14\ \mathrm{keV})$ G. This field estimate is much greater than that derived from the spin down of the source, however the burst spectroscopic method measures the field at the surface which can be multipolar, while the spin down measurement is sensitive to the dipolar component.

The feature also could be an electron cyclotron feature at the surface. Replacing m with the electron mass in Eq. 1 we obtain $B = 1.2 \times 10^{12}\,(E/14\ \mathrm{keV})$ G. This field is two orders of magnitude less than the spin down field. However, if the feature occurred higher up in the magnetosphere then the field would be greatly reduced. Thus, an electron cyclotron feature from a burst which occurred in the upper magnetosphere cannot be precluded.

Although these features can, in principle, be proton/electron cyclotron features there are many problems with interpreting them as such. First, it is not clear why three different sources, with different magnetic field strengths would exhibit features with similar energies. Moreover, it is unclear why these features are seldom seen and have not been seen in other high signal-to-noise bursts. Detailed modeling of burst spectra is definitely warranted. The fact that these features occur at similar energies, despite having different magnetic field strengths, may suggest that they are actually atomic lines, and could possibly provide new insights into the composition of the crust and atmosphere of these enigmatic objects.

REFERENCES

1. C. Thompson, and R. C. Duncan, *MNRAS* **275**, 255–300 (1995).
2. C. Thompson, and R. C. Duncan, *ApJ* **473**, 322–342 (1996).
3. F. P. Gavriil, V. M. Kaspi, and P. M. Woods, *Nature* **419**, 142–144 (2002).
4. V. M. Kaspi, F. P. Gavriil, P. M. Woods, J. B. Jensen, M. S. E. Roberts, and D. Chakrabarty, *ApJ* **588**, L93 (2003).
5. P. M. Woods, C. Kouveliotou, F. P. Gavriil, Kaspi, V. M., M. S. E. Roberts, A. Ibrahim, C. B. Markwardt, J. H. Swank, and M. H. Finger, *ApJ* **629**, 985–997 (2005).
6. H. Krimm, S. Barthelmy, S. Campana, J. Cummings, G. Israel, D. Palmer, and A. Parsons, *The Astronomer's Telegram* **894**, 1–+ (2006).
7. P. M. Woods, and C. Thompson, "Soft Gamma Repeaters and Anomalous X-ray Pulsars: Magnetar Candidates," in *Compact Stellar X-ray Sources*, edited by W. H. G. Lewin, and M. van der Klis, Cambridge University Press, UK, 2006.
8. C. Thompson, M. Lyutikov, and S. R. Kulkarni, *ApJ* **574**, 332–355 (2002).
9. M. Lyutikov, *ApJ* **580**, L65 (2002).
10. F. P. Gavriil, V. M. Kaspi, and P. M. Woods, *ApJ* **641**, 418–426 (2006).
11. P. M. Woods, C. Kouveliotou, E. Göğüş, M. H. Finger, J. Swank, D. A. Smith, K. Hurley, C. Thompson, *ApJ* **552**, 748–755 (2001).
12. P. M. Woods, V. M. Kaspi, C. Thompson, F. P. Gavriil, H. L. Marshall, D. Chakrabarty, K. Flanagan, J. Heyl, and L. Hernquist, *ApJ* **605**, 378–399 (2004).
13. W. Zhu, V. M. Kaspi, P. M. Woods, F. P. Gavriil, R. Dib, *ApJ* (2007), arXiv: 0710.1896 (astro-ph)
14. F. P. Gavriil, and V. M. Kaspi, *ApJ* **609**, L67–L70 (2004).
15. C. R. Tam, F. P. Gavriil, R. Dib, V. M. Kaspi, P. M. Woods, and C. Bassa, *ApJ* (2007), arXiv:0707.2093(astro-ph).
16. R. Dib, V. M. Kaspi, and F. P. Gavriil, *ApJ* **666**, 1152–1164 (2007).
17. F. P. Gavriil, V. M. Kaspi, and P. M. Woods, *ApJ* **607**, 959–969 (2004).
18. S. K. Patel, C. Kouveliotou, P. M. Woods, A. F. Tennant, M. C. Weisskopf, M. H. Finger, C. A. Wilson, E. Göğüş, M. van der Klis, and T. Belloni, *ApJ* **587**, 367–372 (2003).
19. M. Durant, and M. H. van Kerkwijk, *ApJ* **650**, 1082–1090 (2006).
20. M. E. Gonzalez, R. Dib, V. M. Kaspi, P. M. Woods, C. R. Tam, and F. P. Gavriil, *ApJ* (2007), arXiv: 0708.2756 (astro-ph).